

Interstitial-mediated mechanisms of As and P diffusion in Si: Gradient-corrected density-functional calculations

Scott A. Harrison, Thomas F. Edgar, and Gyeong S. Hwang*

Department of Chemical Engineering, University of Texas, Austin, Texas 78713, USA

(Received 3 July 2006; published 7 November 2006)

Gradient-corrected density-functional calculations are used to determine the structure, stability, and diffusion of arsenic-interstitial and phosphorus-interstitial pairs in the positive, neutral, and negative charge states. For both cases, our calculations show that the neutral pair will be dominant under intrinsic conditions while the neutral and negative pairs will both be important in extrinsic n -type materials. The overall diffusion activation energies of neutral $\text{As}_s\text{-Si}_i$ and $\text{P}_s\text{-Si}_i$ pairs are predicted to be 3.75 eV and 3.43 eV, respectively, in good agreement with experimental observations in intrinsic regions.

DOI: [10.1103/PhysRevB.74.195202](https://doi.org/10.1103/PhysRevB.74.195202)

PACS number(s): 61.72.-y, 66.30.-h, 71.15.Mb

I. INTRODUCTION

According to the 2005 Semiconductor Industry Association (SIA) International Technology Roadmap for Semiconductors (ITRS), scaling complementary metal oxide semiconductor (CMOS) devices beyond the 45-nm node in 2010 may require the formation of highly doped ultrashallow junctions less than 7 nm deep with high lateral abruptness. To meet these stringent requirements, it is necessary to have a better understanding of the underlying mechanisms of transient enhanced diffusion (TED) and deactivation of implanted dopants during postimplantation annealing.

It is now well accepted that dopant diffusion is mainly mediated by native defects created in the substrate. For commonly used n -type dopants, arsenic (As) and phosphorus (P), some early experimental studies suggested that As TED could be mediated by both interstitials and vacancies while P TED would be exclusively mediated by interstitials.^{1,2} In addition, recent experimental studies³⁻⁵ also demonstrated the important role of interstitials in driving As TED. However, previous first principles studies mainly focused on understanding the vacancy-mediated diffusion mechanisms of As (Refs. 6–8) and P (Ref. 9). Only recently, some density functional calculations have been undertaken to examine atomistic mechanisms for the interstitial-mediated diffusion of As (Ref. 10) and P (Ref. 11) in Si.

In this paper, we revisit mechanisms for interstitial-mediated diffusion of As and P atoms using first principles quantum mechanical calculations. Here, we attempt to accurately determine local-minimum configurations of $\text{As}_s\text{-Si}_i$ and $\text{P}_s\text{-Si}_i$ pairs in various charge states, and their relative binding strength as well as lowest-energy diffusion pathways and barriers. The subscripts s and i indicate substitutional and interstitial, respectively. Results from the first principles calculations can be used to complement existing experimental observations and also clarify the microscopic mechanisms underlying interstitial-mediated As and P diffusion.

II. COMPUTATIONAL DETAILS

All atomic and electronic structures and total energies reported herein were calculated using the plane-wave basis pseudopotential method within the generalized gradient

approximation¹² to density-functional theory (DFT), as implemented in the Vienna *Ab-initio* Simulation Package (VASP).¹³ We use Vanderbilt-type ultrasoft pseudopotentials¹⁴ and a plane-wave cutoff energy of 12 Ry and 16 Ry, respectively, for the As and P systems. The defect systems are modeled using a 216-atom supercell with a fixed lattice constant of 5.457 Å. All atoms were fully relaxed using the conjugate gradient method until residual forces on constituent atoms become smaller than 5×10^{-2} eV/Å. A $(2 \times 2 \times 2)$ k -point mesh in the scheme of Monkhorst-Pack was used for the Brillouin zone sampling.¹⁵ We calculated diffusion barriers and pathways using the nudged elastic band method (NEBM).

We assessed the relative stability of neutral and charged defects by computing defect ionization levels (μ_i). At a given Fermi level (ε_F), the relative formation energy of a charged defect in charge state $q = \pm 1$ to a neutral defect is given by $E_f^q - E_f^0 = q(\varepsilon_F - \mu_i)$, where ε_F is given relative to the valence band maximum (E_V). Thus, the defect levels can be approximated by: $E_D^q + q(E_V^q + \mu_i) = E_D^0$, where E_D^q and E_D^0 are the total energies of the defects in q and neutral charge states, and E_V^q is the position of the valence band maximum in supercell E_D^q . When calculating the total energy of a charged defect, a homogeneous background charge is included to maintain the overall charge neutrality in the periodic supercell. To account for the Coulomb energy between the charged defect and the background charge, a monopole correction is made to the total energy of the charged system.¹⁶ Assuming a pointlike +1 charge defect in the 216-atom supercell, this correction is estimated to be 0.11 eV.

III. RESULTS AND DISCUSSION

A. Arsenic-interstitial ($\text{As}_s\text{-Si}_i$) pairs

We first examined the structure and stability of the $\text{As}_s\text{-Si}_i$ pair in the positive ($\text{As}_s\text{-Si}_i^+$), neutral ($\text{As}_s\text{-Si}_i^0$), and negative ($\text{As}_s\text{-Si}_i^-$) charge states. For the $\text{As}_s\text{-Si}_i^+$ pair, the $\langle 110 \rangle$ -split dumbbell configuration is predicted to be the most stable structure, in which the As and Si atoms are aligned in the (110) direction while sharing a lattice site. The dumbbell structure is only 0.08 eV more stable than interstitial As at the hexagonal site, resembling the structure of the neutral Si

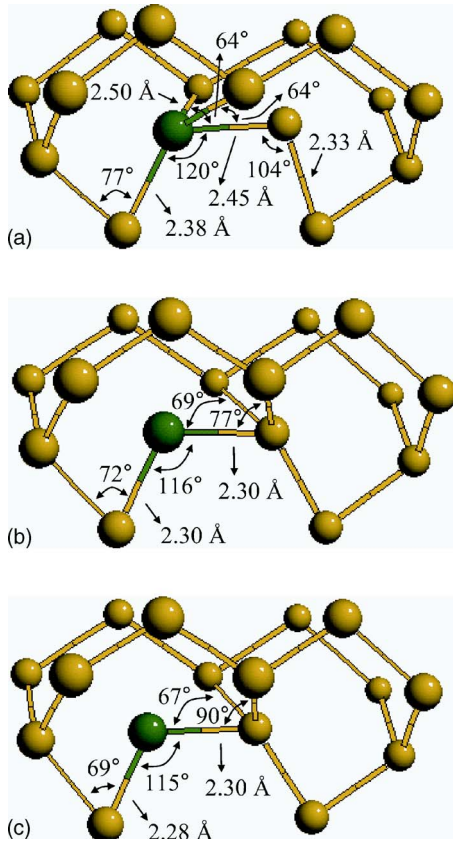


FIG. 1. (Color online) Predicted lowest-energy configurations of (a) positive $As_s-Si_i^+$, (b) neutral $As_s-Si_i^0$, and (c) negative $As_s-Si_i^-$ pairs. The green (dark-colored) and yellow (light-colored) balls represent As and Si atoms, respectively.

interstitial. For the $As_s-Si_i^-$ pair, the As atom is covalently bonded to two adjacent Si lattice atoms while having two electron lone pairs. Our calculations also predict that the most stable structure of $As_s-Si_i^0$ is similar to that of $As_s-Si_i^-$, albeit slightly (~ 0.03 eV) more stable than the $\langle 110 \rangle$ -split dumbbell structure. The bond lengths and angles of the As_s-Si_i pairs are shown in Fig. 1.

Our calculation predicts the relative formation energy of the neutral $As_s-Si_i^0$ pair to be 3.04 eV with respect to neutral As_s^0 ; that is,

$$E_f(As_s - Si_i^0) = E[AsSi_{216}] - E[AsSi_{215}] - E[Si_{216}]/216,$$

where $E[AsSi_{216}]$, $E[AsSi_{215}]$, and $E[Si_{216}]$ are the total energies of 216-atom supercells that contain $As_s-Si_i^0$, As_s^0 , and no defect, respectively. Considering the actual Si bandgap of 1.12 eV and the first As donor level (+/0) of 0.049 eV,¹⁷ under intrinsic conditions at room temperature we can expect that the $As_s-Si_i^0$ formation energy will be as high as 3.55 eV ($=3.04+0.51$) with respect to the As_s ground state As_s^+ . While uncertainty exists in the DFT values of ionization levels, our DFT-GGA calculations predict the first donor and acceptor levels of the As_s-Si_i pair to be $E_V+0.14$ eV and $E_V+0.46$ eV, respectively, for the computed Si bandgap of

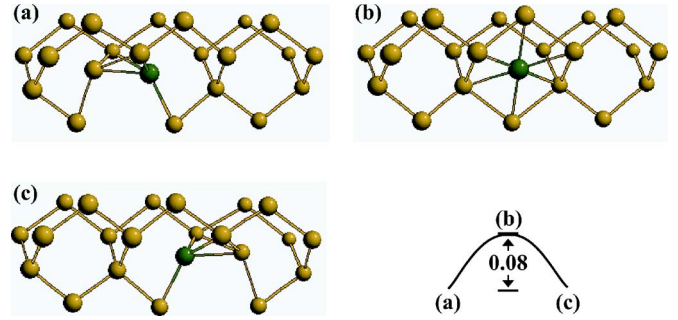


FIG. 2. (Color online) Predicted lowest-energy diffusion pathway of the positive $As_s-Si_i^+$ pair, together with an energy variation along the path. The green (dark-colored) and yellow (light-colored) balls represent As and Si atoms, respectively.

0.63 eV. This suggests that $As_s-Si_i^0$ pairs can be prevailing at midgap while $As_s-Si_i^-$ pairs are expected to be energetically favorable in highly As doped (extrinsic) regions.

Taking the computed relative formation energies, the $As_s-Si_i^0$ binding energy is estimated to be 0.66 eV, relative to the neutral products, As_s^0 and Si_i^0 ; that is, $E_b(As_s-Si_i^0) = E_f(As_s^0) + E_f(Si_i^0) - E_f(As_s-Si_i^0)$, where $E_f(As_s^0)$ is set to zero and $E_f(Si_i^0)$ is 3.70 eV. Here, we consider the $\langle 110 \rangle$ -split dumbbell interstitial (which turns out to be the most favorable structure at the neutral state). If the likely dissociation into As_s^+ and Si_i^0 is considered, the $As_s-Si_i^0$ binding energy in intrinsic regions at room temperature may decrease as far as 0.15 eV ($=0.66-0.51$) (given that the formation energy difference between As_s^+ and As_s^0 can be 0.51 eV in the actual midgap level of Si). However, in an As-doped (extrinsic) region, the $As_s-Si_i^0$ binding energy will increase linearly as the Fermi level shifts towards the conduction band edge. Furthermore, the negative $As_s-Si_i^-$ pair is expected to become important when the Fermi level position is above the first $As-Si_i$ acceptor level, resulting in a further increase in the binding strength of As_s-Si_i pairs. That is, assuming Si_i^0 is the most favorable interstitial above midgap, the As_s-Si_i binding energy can be in a range between 0.15 eV and $(0.66+E_g-E_A)$ eV, where E_g and E_A are the actual Si band gap and the actual first As_s-Si_i acceptor level, respectively.

Next, we investigated the diffusion pathways and barriers for As_s-Si_i pairs. The results are shown in Figs. 2–4: For the

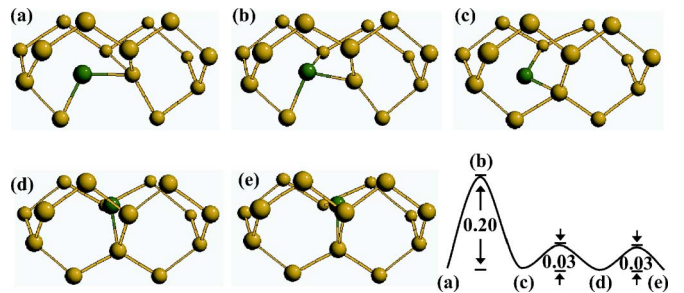


FIG. 3. (Color online) Predicted lowest-energy diffusion pathway of the neutral $As_s-Si_i^0$ pair, together with an energy variation along the path. The green (dark-colored) and yellow (light-colored) balls represent As and Si atoms, respectively.

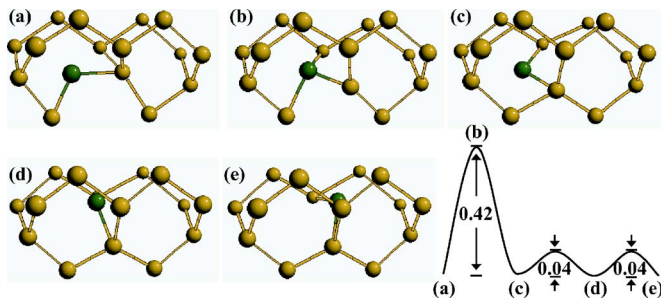


FIG. 4. (Color online) Predicted lowest-energy diffusion pathway of the negative $\text{As}_s\text{-Si}_i^-$ pair, together with an energy variation along the path. The green (dark-colored) and yellow (light-colored) balls represent As and Si atoms, respectively.

$\text{As}_s\text{-Si}_i^+$ pair, as illustrated in Fig. 2, the high energy transition in which As occupies a hexagonal site [(b)] is only 0.08 eV above the lowest-energy structure [(a)]. From the hexagonal state [(b)], the As atom has the potential to migrate in six different directions.

For the $\text{As}_s\text{-Si}_i^0$ pair (see Fig. 3), the initial step involves As migration from one bridged site [(a)] to another [(c)] by breaking an As-Si bond and forming a new As-Si bond. The transition state [(b)] for this step was found to be 0.20 eV above the initial state [(a)]. The next two migration steps from (c) to (d) and from (d) to (e) involve As reorientation within the same bridged site by overcoming negligible energy barriers.

As shown in Fig. 4, the $\text{As}_s\text{-Si}_i^-$ pair diffusion pathway is nearly identical to that for the $\text{As}_s\text{-Si}_i^0$ pair, except that the transition state [(b)] is 0.42 eV above its respective ground state [(a)]. In contrast to the diffusion pathways shown in Figs. 3 and 4, the competing pathways for $\text{As}_s\text{-Si}_i^0$ and $\text{As}_s\text{-Si}_i^-$ pair diffusion in which As migrates through a hexagonal site were found to cost 0.52 eV and 0.94 eV, respectively. In both cases, this competing pathway is highly unfavorable.

According to our predicted formation energies, the As-Si_i^0 pair will be the dominant diffusion component under intrinsic conditions while both As-Si_i^0 and As-Si_i^- pairs may contribute comparably to As diffusion under extrinsic conditions. For the neutral case, the activation energy (given as the formation energy plus the diffusion barrier) is predicted to be 3.75 eV ($=3.55+0.20$), with respect to the As ground state As_s^+ . While no experimental observation is available for direct comparison, the calculated activation energy is in good agreement with 3.81 eV as determined from recent experiments for intrinsic As diffusion at high temperatures ($\approx 900\text{--}1200^\circ\text{C}$).¹⁸ Much earlier experimental studies¹ also reported activation energies of about 4.0 eV for As diffusion in Si. Here, it is important to note that those experiments^{1,18} were conducted under equilibrium conditions in which vacancy and interstitial populations would be nearly equal. Hence, under such conditions we expect that both vacancies and interstitials can mediate As diffusion. Indeed, previous DFT studies⁸ also predicted the activation energy of 3.56 eV for neutral As-V pair diffusion, close to the experimental values, while As-V pairs have been found to undergo diffusion by a ring mechanism.⁶⁻⁸

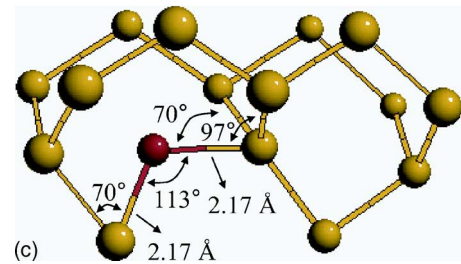
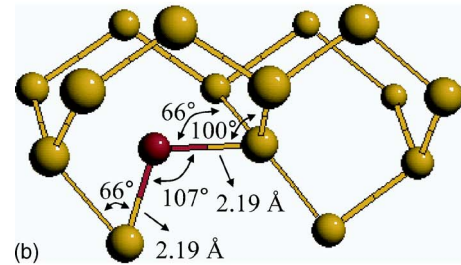
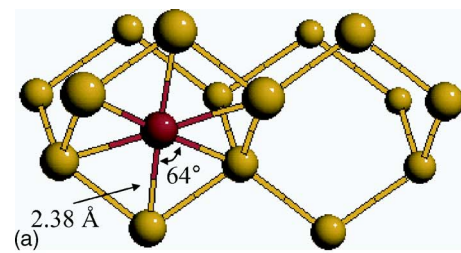


FIG. 5. (Color online) Predicted lowest-energy configurations of (a) positive $\text{P}_s\text{-Si}_i^+$ (b) neutral $\text{P}_s\text{-Si}_i^0$ and (c) negative $\text{P}_s\text{-Si}_i^-$ pairs. The red (dark-colored) and yellow (light-colored) balls represent P and Si atoms, respectively.

B. Phosphorus-interstitial ($\text{P}_s\text{-Si}_i$) pairs

Figure 5 shows the lowest-energy configuration of $\text{P}_s\text{-Si}_i$ pairs in the positive, neutral, and negative charge states. For $\text{P}_s\text{-Si}_i^+$ and $\text{P}_s\text{-Si}_i^0/\text{P}_s\text{-Si}_i^-$ pairs, the P atom occupies a hexagonal site and a bond-center site, respectively. The relative formation energy for $\text{P}_s\text{-Si}_i^0$ pair is predicted to be 2.74 eV with respect to P_s^0 , which is given in a similar manner as for the $\text{As}_s\text{-Si}_i^0$ pair with $E_f(\text{P}_s^0)=0$ eV and $E_f(\text{Si}_i^0)=3.70$ eV. Taking the actual Si bandgap of 1.12 eV and the first P donor level of 0.045 eV,¹⁷ the $\text{P}_s\text{-Si}_i^0$ formation energy is computed to be 3.25 eV ($=2.74+0.51$) with respect to P_s^+ at room temperature. For the computed Si bandgap of 0.63 eV, the first donor and acceptor level of $\text{P}_s\text{-Si}_i$ are determined to be $E_V+0.22$ and $E_V+0.42$, respectively. While uncertainty exists in the ionization levels, our results show that $\text{P}_s\text{-Si}_i^0$ pairs will be favorable at midgap ($=E_V+0.315$) while $\text{P}_s\text{-Si}_i^-$ pairs will become important under highly P doped (extrinsic) conditions.

Taking the formation energies, relative to the neutral products P_s^0 and (110)-split Si_i^0 , the binding energy of $\text{P}_s\text{-Si}_i^0$ is determined to be 0.96 eV [$=E_f(\text{P}_s^0)+E_f(\text{Si}_i^0)-E_f(\text{P}_s\text{-Si}_i^0)$, where $E_f(\text{P}_s^0)$ is set to zero and $E_f(\text{Si}_i^0)$ is 3.70 eV]. Note that the $\text{P}_s\text{-Si}_i$ binding is 0.3 eV stronger than the $\text{As}_s\text{-Si}_i$ case. If the likely dissociation into P_s^+ and Si_i^0 is considered, the $\text{P}_s\text{-Si}_i^0$ binding energy may lower as far as

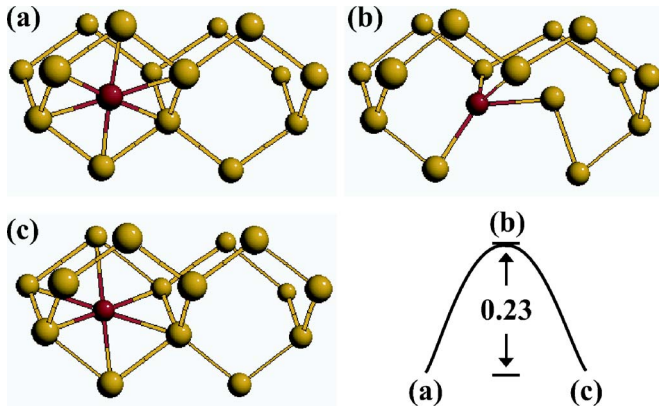


FIG. 6. (Color online) Predicted lowest-energy diffusion pathway of the positive $P_s\text{-Si}_i^+$ pair, together with an energy variation along the path. The red (dark-colored) and yellow (light-colored) balls represent P and Si atoms, respectively.

0.45 eV ($=0.96-0.51$) in intrinsic regions at room temperature. However, the $P_s\text{-Si}_i$ binding strength with respect to P_s^+ and Si_i^0 will increase as the Fermi level shifts towards the conduction band edge in heavily P-doped regions. Similar to the case for $\text{As}_s\text{-Si}_i$ pairs, the negative $P_s\text{-Si}_i^-$ pair is expected to become important when the Fermi level position is above the first P-Si_i acceptor level. At such elevated Fermi level positions, the binding energy for the $P_s\text{-Si}_i^-$ pair would exceed that of the $P_s\text{-Si}_i^0$ pair. That is, suppose (110)-split Si_i^0 is the ground state above midgap, the $P_s\text{-Si}_i$ binding energy is predicted to range from 0.45 eV to $(0.96+E_g-E_A)$ eV in P-doped Si, where E_g and E_A are the actual Si gap and the actual first $P_s\text{-Si}_i$ acceptor level, respectively.

Figures 6–8 show the migration pathways and barriers for the $P_s\text{-Si}_i^+$, $P_s\text{-Si}_i^0$, and $P_s\text{-Si}_i^-$ pairs. During $P_s\text{-Si}_i^+$ pair diffusion (see Fig. 6), P migrates from one ground-state hexagonal site [(a)] to another [(c)] via a dumbbell-like saddle point [(b)] which is 0.23 eV higher in energy than the ground state. The $P_s\text{-Si}_i^+$ diffusion behavior is consistent with previous theoretical predictions.¹¹

As shown in Figs. 7 and 8, the diffusion of $P_s\text{-Si}_i^0$ and $P_s\text{-Si}_i^-$ follows a similar pathway as for $\text{As}_s\text{-Si}_i^0$ and $\text{As}_s\text{-Si}_i^-$ (Figs. 3 and 4). The overall diffusion barriers for the neutral and negative pairs are predicted to be 0.18 eV and 0.43 eV, respectively. For each pair, the identified mecha-

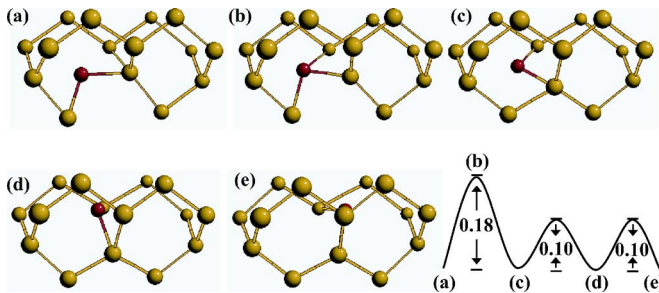


FIG. 7. (Color online) Predicted lowest-energy diffusion pathway of the neutral $P_s\text{-Si}_i^0$ pair, together with an energy variation along the path. The red (dark-colored) and yellow (light-colored) balls represent P and Si atoms, respectively.

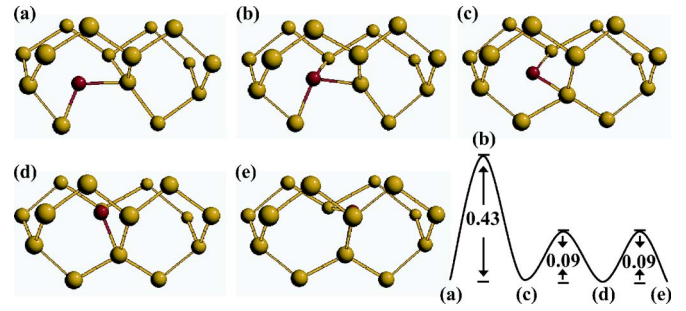


FIG. 8. (Color online) Predicted lowest-energy diffusion pathway of the negative $P_s\text{-Si}_i^-$ pair, together with an energy variation along the path. The red (dark-colored) and yellow (light-colored) balls represent P and Si atoms, respectively.

nism gives a far lower barrier than another competing mechanism that involves P migration through a hexagonal site which requires overcoming barriers of 0.37 (0.6) eV and 0.87 (1.4) eV, respectively, for $P_s\text{-Si}_i^0$ and $P_s\text{-Si}_i^-$ pairs from our¹¹ DFT-GGA calculations. Looking at the sizable barrier difference, we expect that the identified pathway will be favorable in $P_s\text{-Si}_i^0$ and $P_s\text{-Si}_i^-$ diffusion (when no charge variation is allowed).

Similar to the $\text{As}_s\text{-Si}_i$ case, the predicted formation energies suggest that the $P_s\text{-Si}_i^0$ pair will be the dominate diffusing component under intrinsic conditions while $P_s\text{-Si}_i^0$ and $P_s\text{-Si}_i^-$ pairs can both contribute comparably to diffusion under n -type extrinsic conditions. For the neutral case, the diffusion activation energy (given as the formation energy plus the diffusion barrier) is predicted to be 3.43 eV ($=3.25+0.18$), with respect to the P ground state P_s^+ . Our result is consistent with an earlier DFT study that predicted the $P_s\text{-Si}_i^0$ pair to have an activation energy of 3.1–3.5 eV.¹¹ From experiments conducted under equilibrium conditions, P diffusion activation energies of 3.30 eV,¹⁹ 3.69 eV,²⁰ 3.55 eV,²¹ 3.61 (high temperature) and 2.81 eV (low temperature),²² 2.74 eV,²³ and 2.65 eV (Ref. 24) have been extracted. While there is some variation in the experimentally derived values for activation energy, the predicted value of 3.43 eV for $P_s\text{-Si}_i^0$ pair diffusion falls within the range of these reported experimental values.

IV. CONCLUSIONS

Using DFT-based first principles calculations, we determined local-minimum configurations of $\text{As}_s\text{-Si}_i$ and $P_s\text{-Si}_i$ pairs in the positive, neutral, and negative charge states, along with their binding energies and lowest-energy diffusion pathways and barriers. For the $\text{As}_s\text{-Si}_i^+$ pair, the $\langle 110 \rangle$ -split dumbbell configuration is predicted to be the most stable structure, whereas interstitial P at the hexagonal site turns out to be the most stable configuration for the $P_s\text{-Si}_i^+$ pair. For both neutral and negative pairs, on the other hand, in the ground-state structure, the As/P atom is covalently bonded to two Si lattice atoms, breaking the Si-Si bond that would otherwise exist in a perfect Si crystal. Our calculations predict the first donor and acceptor levels of the $\text{As}_s\text{-Si}_i/P_s\text{-Si}_i$ pair to be $E_V+0.14/0.22$ eV and E_V

+0.46/0.42 eV, respectively, for the computed Si bandgap of 0.63 eV. This suggests that for both As and P the neutral pair can be prevailing in intrinsic regions while the negative pair becomes important under n -type extrinsic conditions. In n -type materials, the binding energies of $\text{As}_s\text{-Si}_i/\text{P}_s\text{-Si}_i$ pairs are predicted to range from 0.15/0.45 eV to $(0.66/0.96+E_g-E_A)$ eV, where E_g and E_A are the actual Si band gap and the actual first $\text{As}_s\text{-Si}_i/\text{P}_s\text{-Si}_i$ acceptor level, respectively. We also find that both neutral and negatively charged As-Si_i and P-Si_i pairs diffuse by an identical pathway in which the dopant is bond centered at energy minima and threefold coordinated at the high energy saddle point. The predicted overall activation energies of 3.75 eV and 3.43 eV for As-Si_i^0 and P-Si_i^0 diffusion are in good agree-

ment with experimental observations in intrinsic regions, supporting the idea that interstitials play an important role in As and P diffusion in Si.

ACKNOWLEDGMENTS

G.S.H. gratefully acknowledges the Welch Foundation (F-1535) and the National Science Foundation (CAREER-CTS-0449373 and ECS-0304026) for their partial financial support. S.A.H. would like to thank the NSF and the University of Texas for support. We would also like to thank the Texas Advanced Computing Center for use of their computing resources.

*Author to whom correspondence should be addressed. Electronic address: gshwang@che.utexas.edu

- ¹P. M. Fahey, P. B. Griffin, and J. D. Plummer, *Rev. Mod. Phys.* **61**, 289 (1989).
- ²A. Ural, P. B. Griffin, and J. D. Plummer, *J. Appl. Phys.* **85**, 6440 (1999).
- ³S. Solmi, M. Ferri, M. Bersani, D. Giubertoni, and V. Soncini, *J. Appl. Phys.* **94**, 4950 (2003).
- ⁴R. Kim, T. Hirose, T. Shano, H. Tsuji, and K. Taniguchi, *Jpn. J. Appl. Phys., Part 1* **41**, 227 (2002).
- ⁵C. Tsamis, D. Skarlatos, G. BenAssayag, A. Claverie, W. Lerch, and V. Valamontes, *Appl. Phys. Lett.* **87**, 201903 (2005).
- ⁶M. Ramamoorthy and S. T. Pantelides, *Phys. Rev. Lett.* **76**, 4753 (1996).
- ⁷O. Pankratov, H. Huang, T. Diaz de la Rubia, and C. Mailhot, *Phys. Rev. B* **56**, 13172 (1997).
- ⁸J. J. Xie and S. P. Chen, *Phys. Rev. Lett.* **83**, 1795 (1999).
- ⁹J. S. Nelson, P. A. Schultz, and A. F. Wright, *Appl. Phys. Lett.* **73**, 247 (1998).
- ¹⁰S. A. Harrison, T. F. Edgar, and G. S. Hwang, *Appl. Phys. Lett.* **87**, 231905 (2005).
- ¹¹X. Y. Liu, W. Windl, K. M. Beardmore, and M. P. Masquelier,

- Appl. Phys. Lett.* **82**, 1839 (2003).
- ¹²J. P. Perdew and Y. Wang, *Phys. Rev. B* **45**, 13244 (1992).
- ¹³G. Kresse and J. Furthmuller, *Phys. Rev. B* **54**, 11169 (1996).
- ¹⁴D. Vanderbilt, *Phys. Rev. B* **41**, 7892 (1990).
- ¹⁵H. J. Monkhorst and J. D. Pack, *Phys. Rev. B* **13**, 5188 (1976).
- ¹⁶G. Makov and M. C. Payne, *Phys. Rev. B* **51**, 4014 (1995).
- ¹⁷C. Kittel, *Introduction to Solid State Physics*, 7th ed. (Wiley, Hoboken, NJ, 1996).
- ¹⁸P. Laitinen, I. Riihimäki, and J. Räisänen, *Phys. Rev. B* **68**, 155209 (2003).
- ¹⁹R. N. Ghoshtagore, *Phys. Rev. B* **3**, 397 (1971).
- ²⁰J. S. Makris and B. J. Masters, *J. Electrochem. Soc.* **120**, 1252 (1973).
- ²¹A. Ural, P. B. Griffin, and J. D. Plummer, *Phys. Rev. Lett.* **83**, 3454 (1999).
- ²²Y. M. Haddara, B. T. Folmer, M. E. Law, and T. Buyuklimanli, *Appl. Phys. Lett.* **77**, 1976 (2000); references cited therein.
- ²³J. S. Christensen, H. H. Radamson, A. Y. Kuznetsov, and B. G. Svensson, *Appl. Phys. Lett.* **82**, 2254 (2003).
- ²⁴A. Nylandsted Larsen, N. Zangenberg, and J. Fage-Pedersen, *Mater. Sci. Eng., B* **124-125**, 241 (2005).